https://doi.org/10.1016/j.commatsci.2021.110843

A novel two-stage martensitic transformation induced by nanoscale concentration modulation in a TiNb-based shape memory alloy

Jiaming Zhu[a,*], Gang Zhang[b], He Huang[c], Dong Wang[d], Peijian Chen[e,*], Xusheng Yang[f,g*]

[a] School of Civil Engineering, Shandong University, Jinan 250061, China

[b] Institute of Physics and Optoelectronics Technology, Baoji University of Arts and Sciences, Baoji 721016, China

[c] School of Materials Science and Engineering, University of Science and Technology Beijing, Beijing 100083, China

[d] Center of Microstructure Science, Frontier Institute of Science and Technology, Xi'an Jiaotong University, Xi'an 710049, China

[e] State Key Laboratory for Geomechanics and Deep Underground Engineering, School of Mechanics and Civil Engineering, China University of Mining and Technology, Xuzhou, Jiangsu, 221116, China

[f] State Key Laboratory of Ultra-precision Machining Technology, Department of Industrial and Systems Engineering, The Hong Kong Polytechnic University, Hung Hom, Kowloon, Hong Kong, China

[g] Hong Kong Polytechnic University Shenzhen Research Institute, Shenzhen, China

Abstract

Martensitic transformation (MT) plays a critical role in determining both mechanical and functional properties of shape memory alloys (SMAs). The behavior of MT depends strongly on the microstructure of materials, and two- or multiple-stage MTs are typical examples of this. However, the physical origin of two- or multiple-stage MTs remains controversial although much effort has been made. In this study, a novel two-stage MT is observed in a TiNb-based SMA with nanoscale concentration modulation. The physical origin of this chemical-heterogeneity-induced two-stage MT is the difference in thermodynamic stability of the parent and martensitic phase between Nb-leaner and Nb-richer regions. The findings of this study not only expand the repertoire of mechanisms of two- or multiple-stage MT but also shed light on the long-standing controversy over the physical origin of multiple-stage MTs.

Keywords: Two-stage martensitic transformation, Concentration modulation, Shape memory alloy, Phase field method

Corresponding Authors:

Jiaming Zhu, E-mail: zhujiaming@sdu.edu.cn

Peijian Chen, E-mail: chenpeijian@cumt.edu.cn

Xusheng Yang, E-mail: xsyang@polyu.edu.hk

1. Introduction

As the physical origin of the shape memory effect and super-elasticity of shape memory alloys (SMAs), the behavior of martensitic transformations (MTs) determines the performance of SMAs [1]. In most SMAs, MTs show a fisrt-order phase transition behavior [2], making SMAs exhibit large phase transformation hysteresis and strong non-linear deformation behavior. These mechanical properties limit the performance of SMA devices in various applications although they are useful in some areas [3]. For example, the large hysteresis lowers the efficiency of actuators and solid cooling devices [3], and the strong non-linear deformation behavior makes precise position control of actuators difficult [4]. Therefore, much effort has been made to enhance the mechanical properties of SMAs via tuning the kinetic process of MTs.

Structural heterogeneities are widely used to change the MT behavior. For example, it has been reported that point defects [5–7], stress-carrying dislocations [8] and nanosized precipitates [9,10] could transform MTs from first-order to continuous. Moreover, the effect of nanocrystallization on MTs has also been studied [11–15]. It is noteworthy that structural heterogeneities may influence not only the first-order feature of MTs but also the MT path by inducing multiple-stage MTs, rendering obvious change in both mechanical and functional properties of SMAs [2]. For example, it is well documented that the appearance of Ni_4Ti_3 precipitates changes the original B2→B19′ MT to B2→R→B19′ MT in NiTi alloys and that the B2→R→B19′ MT usually occurs via a multiple-stage manner because of the structural heterogeneity in matrix [16,17]. It is noteworthy that, according to Bataillard et al. [18], a two- or multiple-stage MT may result from the appearance of intermediate phases or the split of transformation process, i.e. asynchronous transformation of different regions of the parent phase.

Up to now, two- or multiple-stage MTs are reported mainly in nitinol and is assumed to stem from structural heterogeneity induced by precipitates [16]. In contrast, a novel two-stage MT induced by chemical heterogeneity, i.e. concentration modulation (CM), is found in a TiNb-based SMA via computer modeling based on phase field method in this study. The findings of this study not only extend the repertoire of two- or multiple-stage MTs but also provide insights into the physical origin of multiple-stage MTs and the control of MT via CM.

2. Development of phase field model

To study the behavior of MT in systems with chemical heterogeneity, a nanoscale CM (i.e. the concentration of Nb varies between 8 at.% and 20 at.%) is first developed in Ti2448 (Ti-24Nb-4Zr-

8Sn-0.10O in wt.%) [19] via spinodal decomposition at 773K, and, then, this CM is used as the input of phase field simulations of MT which is triggered by applying an uniaxial load at 300K. Phase field models of spinodal decomposition and stress-induced MT are formulated based on a combination of Landau theory [20], gradient thermodynamics [21], and the modified Khachaturyan–Shatalov's microelasticity theory [22,23]. The concentration evolution during spinodal decomposition is governed by the Cahn-Hilliard equation [24], and the temporal and spatial evolution of the structural order parameters (which represent the parent and martensitic phases) during MT are described by the time-dependent Ginzburg-Landau equation [25–28]. The symmetry breaking accompanying the β (BCC, point group $m\bar{3}m$) $\rightarrow$ α'' (orthorhombic, point group *mmm*) MT [29,30] (see Fig. 1(a)) in TiNb-based SMAs leads to 6 martensitic variants that are crystallographically equivalent but different in orientation [31,32]. In our phase field model, the parent and martensitic phases are described by employing 6 structural order parameters, η_p (p=1~6), with $(\eta_{p=1\sim6} = 0)$ representing the parent phase and $(\eta_p = \pm1,\ \eta_{q=1\sim6,q\neq p} = 0)$ representing the p-th martensitic variant. The dependence of MT on composition (see Fig. 1(b)) is considered by making the Landau free energy of the parent and martensitic phases being composition dependent. The phase field model is validated by comparing simulation results with experimental reports [33–35], as shown in Fig. 1(b)-(c). Fig. 1(c) indicates that the phase field model produces a stress-strain curve that is consistent with the experimental result, in terms of the critical stress for the MT, stress hysteresis, superelasticity and first-order feature of MT, although the simulated curve is not completely coincide with the experimental one. Details on the formulation and validation of the phase field model of both spinodal decomposition and MT can be found in the literature [36]. The size of our simulation box is 128 nm×128 nm×128 nm (see Fig. 2(a)). Periodical boundary conditions are applied along all three dimensions. The global coordinate system in this study parallels to the lattice directions of the parent phase as indicated in Fig. 1(a).

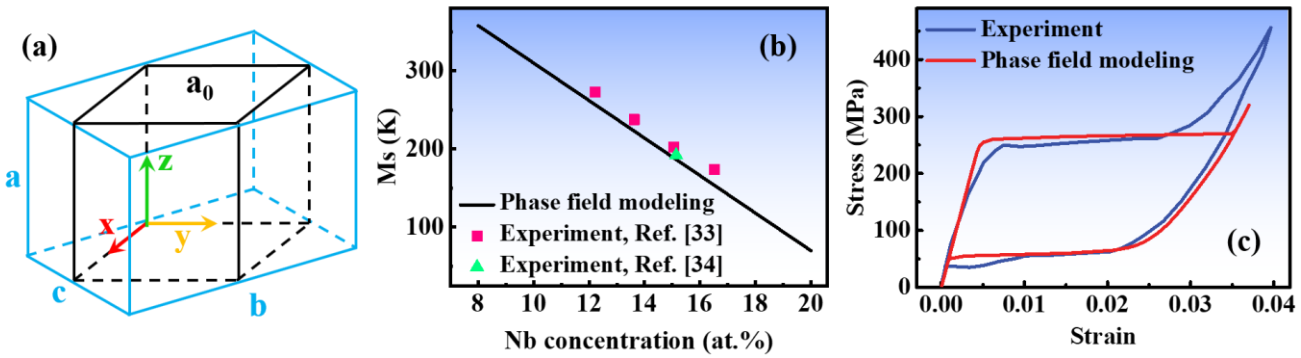

Fig. 1 (a) is a schematic drawing of the lattice correspondence between the β phase (the black one)

and α'' phase (the blue one). The x-y-z coordinate system is the global coordinate system. (b) shows the simulated and experimental results of the composition dependence of martensitic transformation start temperature (M_s). (c) compares the simulated and experimental stress-strain curve of Ti2448.

3. Results and discussion

The three-dimensional (3D) CM obtained from spinodal decomposition by ageing at 773K is shown in Fig. 2(a), and its 1D concentration profile is presented in Fig. 2(b). It should be noted that the ageing temperature is chosen according to experimental results of TiNb binary alloys [37] due to the lack of sufficient experiment data of Ti2448. This estimation is made based on facts that (i) Ti and Nb are principle elements of Ti2448; (ii) the concentration modulation in Ti2448 is induced by the nonuniform distribution of Ti and Nb [19], which is similar to the case in TiNb binary alloys. It is readily seen that CM is well developed in the initial compositionally homogeneous system (with a composition of 15 at.% Nb) and the Nb concentration has reached its equilibrium values (i.e. 8 at.% and 20 at.%) in some regions. The 3D configuration of Nb-lean (~8 at.% Nb) and Nb-rich (~20 at.% Nb) regions are shown in Figs. 2(c)-(d) which, together with Fig. 2(a), demonstrate that Nb-lean and Nb-rich regions occupy a considerable volume fraction of the system. Since MT is sensitive to composition as indicated by Fig. 1(b), it is natural to predict that this CM will change the MT behavior dramatically. To validate this prediction, uniaxial loading is performed on the concentration modulated system.

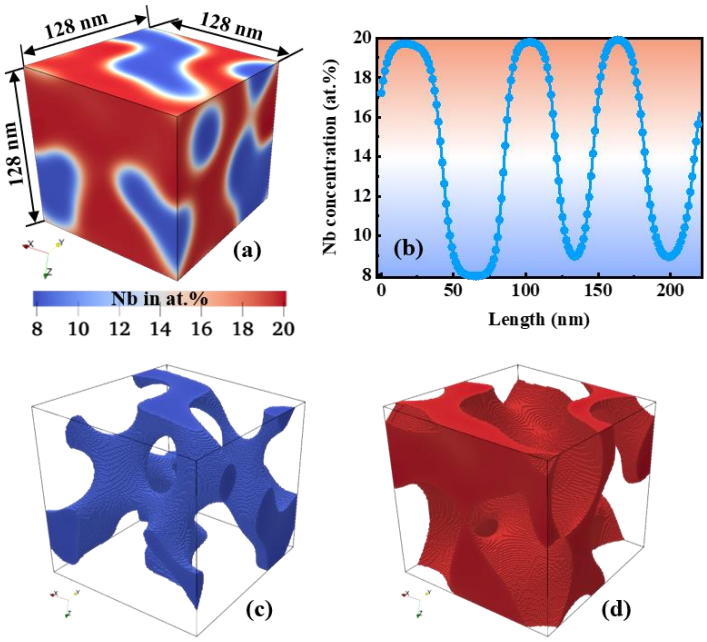

Fig. 2 (a) shows the 3D nanoscale concentration modulation induced by spinodal decomposition. (b)

shows the 1D nanoscale concentration modulation along a body diagonal of the simulation box shown in (a). (c) and (d) show the 3D configuration of regions possessing 8-8.5 at.% Nb and 19.5-20 at.% Nb, respectively.

Fig. 3(a) and 3(b) show the evolution of volume fraction of the α'' phase upon loading and unloading in the concentration modulated system and the compositionally uniform system, respectively. The compositionally uniform system shows a typical square-like curve, i.e. the volume fraction of martensitic phase increases rapidly when external load reaches the critical value and then drops upon unloading. This is consistent with the first-order feature of the $\beta \rightarrow \alpha''$ MT. In contrast, the concentration modulated system exhibites a complex two-stage MT process, i.e. a steep increase of the volume fraction is followed by a gradual increase upon loading. Moreover, the volume fraction of the α'' phase gradually diminishes during unloading, resulting in a much narrower MT hysteresis as compared to the curve in Fig. 3(b). Quantitative analysis to Fig. 3(a) and 3(b) leads to Fig. 3(c) and 3(d), respectively. In these two figures, a parameter

$$\Gamma = dV_M/|d\sigma| \tag{1}$$

is defined to characterized the variation tendency of the volume fraction of martensitic phase, V_M, upon loading and unloading, where $|d\sigma|$ denotes the absolute value of differential $d\sigma$. Therefore, the position, the shape and the number of peaks in the Γ - σ curve reflect features of MT, in analogy to the differential scanning calorimetry (DSC) curve. Peak A and B in Fig. 3(c) clearly demonstrates that the entire MT is mainly divided into two stages. In the first stage, MT shows a first-order feature as indicated by the sharp peak A, while it exhibits a continuous characteristic in the second stage as implied by the broadened and weakened peak B. This two-stage and mixed first-order/continuous behavior distinguishes this MT from the conventional MT shown in Fig. 3(d). It should be pointed out that the yielding phenomenon is not considered in our simulations to investigate the effect of nano-scale CM on MTs. While it should be noted that this simplification does not influence the conclusion of this paper because the critical stress of MT of the Nb-rich region can be reduced by decreasing the test temperature.

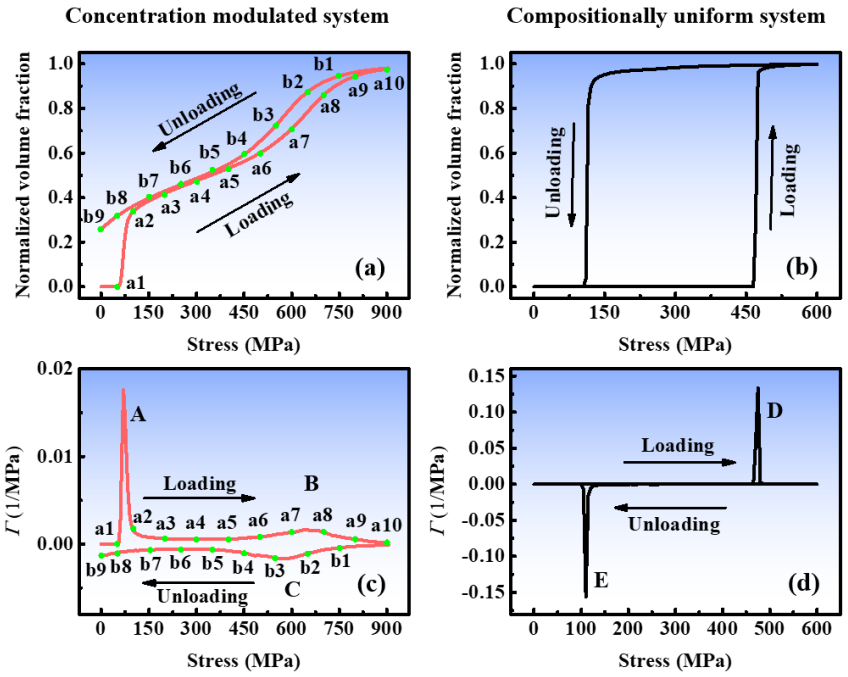

Fig. 3 (a) and (c) show the variation of volume fraction of martensites and Γ value in the concentration modulated system upon uniaxial loading-unloading, respectively. Their counterparts in the compositionally uniform system are shown in (b) and (d), respectively. The definition of Γ can be found in Eq. (1). A positive value of Γ means the volume fraction of martensites increases with the change of external load, and a negative value means the opposite.

To reveal how the CM gives rise to a two-stage MT, the microstructure evolution process of the concentration modulated system upon the forward and backward MT is presented in Fig. 4. It is readily seen that internally-twinned martensitic domains only occupy some regions of the system instead of the entire system. The comparison between Fig. 4(a2) and Fig. 2(a) demonstrates that these transformed regions have a relatively lower Nb concentration. The MT in Nb-leaner regions occurs within a narrow stress window, generating the sharp transformation peak A in Fig. 3(c) and indicating a first-order phase transformation behavior. While these martensitic domains do not expand obviously as the external load increases although the MT in the system is far from complete (see Fig. 4(a3)-(a5)). When the external load reaches 500MPa, martensitic domains start to grow toward Nb-richer regions in a gradual manner (see Fig. 4(a6)-(a10)), which leads to the broadened peak B in Fig. 3(c) and is consistent with the result shown in Fig. 3(a). Upon unloading, backward MT first occurs gradually in Nb-richer regions (see Fig. 4(b1)-(b5)), resulting in the broadened peak C in Fig. 3(c). While martensitic domains in Nb-leaner regions still exist even when the system is completely unloaded because Nb-leaner regions do not reach their critical stress of backward MT. Therefore, only one peak

is observed upon the unloading process.

Fig. 3 and Fig. 4 clearly demonstrate that CM is responsible to the two-stage MT in the concentration modulated system. To reveal the physical origin of this phenomenon, Landau free energies of the Nb-leaner region and Nb-richer region are plotted in Fig. 5. It is readily seen that the Landau free energy of the system is a function of composition. In the Nb-leaner region (e.g. 8 at.%Nb, the red curve), the martensitic phase has a lower free energy than the parent phase and, thus, is thermodynamically more stable than the parent phase. While the situation is opposite in the Nb-richer region. It is the difference in phase stability between Nb-leaner regions and Nb-richer regions that generates an asynchronous transformation, i.e. the observed two-stage MT, in the concentration modulated system.

It is noteworthy that two- and multiple-stage MTs have been reported previously in precipitate-bearing nitinol, which is mainly attributed to the structural heterogeneity induced by precipitates. However, the two-stage MT found in this study is purely due to chemical heterogeneity. Therefore, it is reasonable to predict that two- or multiple-stage MT do not necessarily to be limited to nitinol, instead, they can be expected in other SMAs with CM as well.

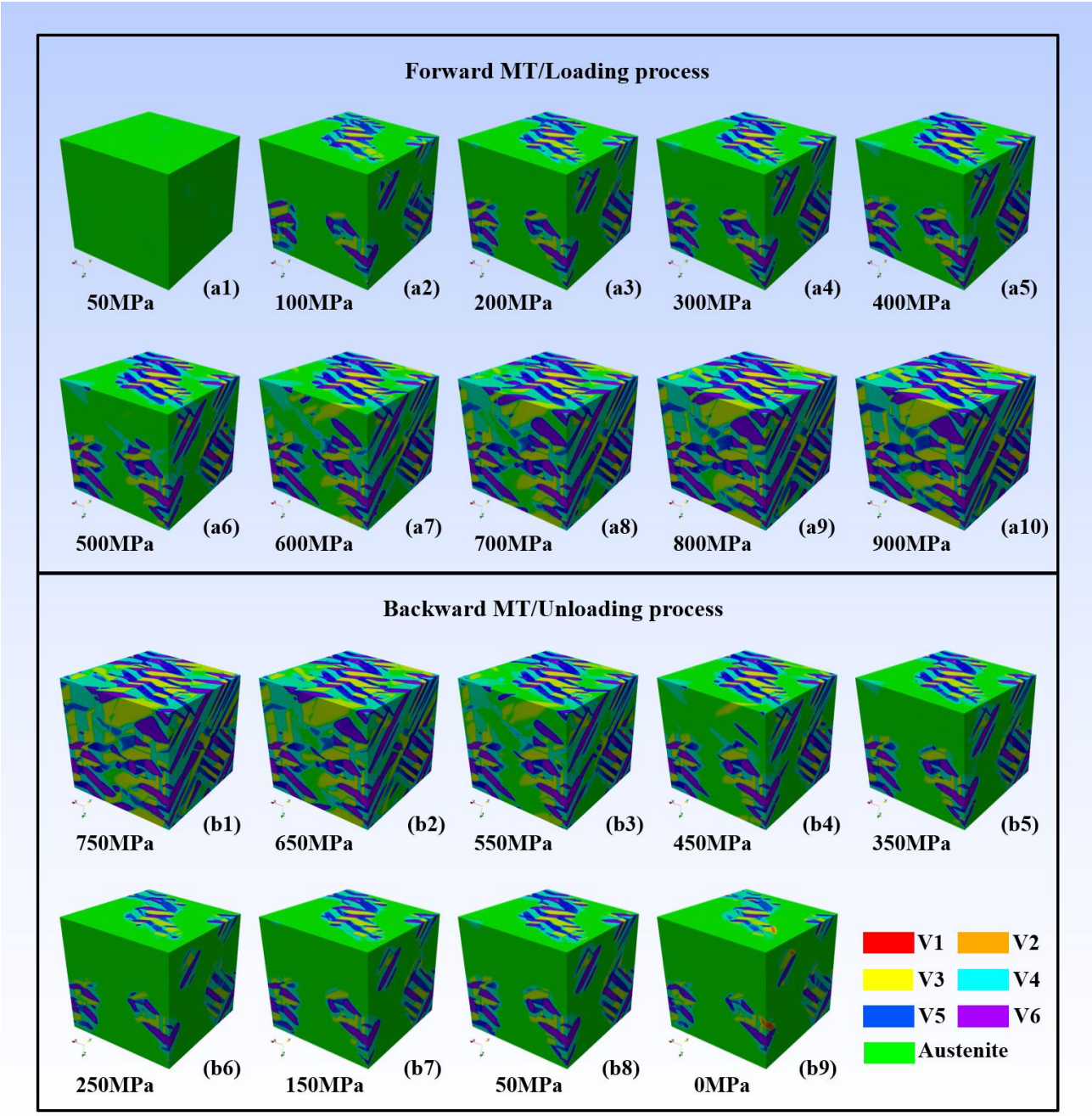

Fig. 4 (a1)-(a10) and (b1)-(b9) show 3D views of microstructure evolution process upon loading and unloading, respectively. Different color represents different phases as indicated at the bottom right corner. The symbol Vn denotes the n-th variant of martentic phase. The locations of these microstructures on the volume fraction curve and Γ - σ curve are marked by green dots in Fig. 3(a) and 3(c).

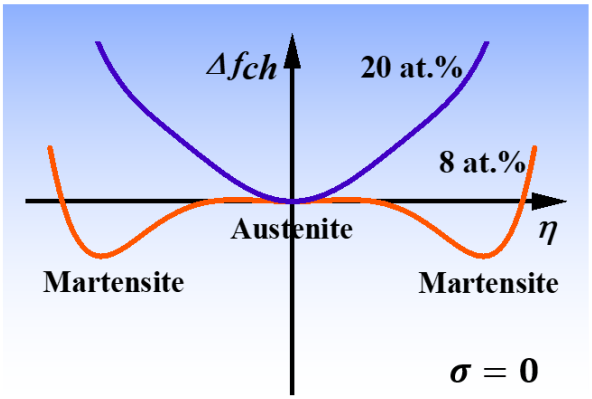

Fig. 5 Landau free energy curves of the Nb-leaner region (8 at.%Nb) and Ni-richer region (20 at.%Nb) at 300 K without external load.

4. Conclusions

In summary, a new two-stage MT is observed in a TiNb-base SMA with CM generated from spinodal decomposition based on phase field modeling. Thermodynamic analyses demonstrate that this two-stage MT originates from the composition dependence of thermodynamic stability of the parent and martensitic phase. The difference in phase stability between Nb-leaner and Nb-richer regions makes MT occurs at different stress levels, resulting in a two-stage MT phenomenon. This chemical-heterogeneity-induced two-stage MT is in sharp contrast to previously reported structural-heterogeneity-induced two- or multiple-stage MT. The findings of this study expand the repertoire of mechanisms of two- or multiple-stage MT and shed light on the long-standing controversy over the physical origin of multiple-stage MTs.

Declaration of Competing Interest

The authors declare that they have no known competing financial interests or personal relationships that could have appeared to influence the work reported in this paper.

Acknowledgement

JZ acknowledges the support of Qilu Young Talent Program from Shandong University and the State Key Lab of Advanced Metals and Materials (Grant No. 2021-Z10). GZ acknowledges the financial support from the Scientific Research Program Funded by Shaanxi Provincial Education Department (Program No. 19JK0039). XY acknowledges the support of the National Natural Science Foundation of China (Grants No. 51701171).

Data Availability

The data that support the findings of this study are available from the corresponding authors upon request.

Reference

[1] K. Bhattacharya, Microstructure of Martensite: Why It Forms and How It Gives Rise to the Shape-Memory Effect, Oxford University Press, Oxford, 2003.

[2] K. Otsuka, X. Ren, Physical metallurgy of Ti-Ni-based shape memory alloys, Prog. Mater. Sci. 50 (2005) 511–678.

[3] J. Mohd Jani, M. Leary, A. Subic, M.A. Gibson, A review of shape memory alloy research, applications and opportunities, Mater. Des. 56 (2014) 1078–1113.

[4] A.T. Tung, B.-H. Park, D.H. Liang, G. Niemeyer, Laser-machined shape memory alloy sensors for position feedback in active catheters, Sensors Actuators A Phys. 147 (2008) 83–92.

[5] D. Wang, Y. Wang, Z. Zhang, X. Ren, Modeling Abnormal Strain States in Ferroelastic Systems: The Role of Point Defects, Phys. Rev. Lett. 105 (2010) 205702.

[6] Y. Zhou, D. Xue, X. Ding, Y. Wang, J. Zhang, Z. Zhang, D. Wang, K. Otsuka, J. Sun, X. Ren, Strain glass in doped Ti50(Ni50−xDx) (D=Co, Cr, Mn) alloys: Implication for the generality of strain glass in defect-containing ferroelastic systems, Acta Mater. 58 (2010) 5433–5442.

[7] D. Wang, Z. Zhang, J. Zhang, Y. Zhou, Y. Wang, X. Ding, Y. Wang, X. Ren, Strain glass in Fe-doped Ti–Ni, Acta Mater. 58 (2010) 6206–6215.

[8] Q. Liang, D. Wang, J. Zhang, Y. Ji, X. Ding, Y. Wang, X. Ren, Y. Wang, Novel B19′ strain glass with large recoverable strain, Phys. Rev. Mater. 1 (2017) 033608.

[9] Y. Ji, X. Ding, T. Lookman, K. Otsuka, X. Ren, Heterogeneities and strain glass behavior: Role of nanoscale precipitates in low-temperature-aged Ti48.7Ni51.3 alloys, Phys. Rev. B. 87 (2013) 104110.

[10] Z. Gao, S. Wang, H.H. Wu, J. Li, X. Mao, Understanding the mismatch strain and orientation of nanoscale second phase on the superelasticity of zirconia, Compos. Commun. 22 (2020) 100521.

[11] J.F. Gómez-Cortés, M.L. Nó, I. López-Ferreño, J. Hernández-Saz, S.I. Molina, A. Chuvilin, J.M. San Juan, Size effect and scaling power-law for superelasticity in shape-memory alloys at the nanoscale, Nat. Nanotechnol. (2017) 1–8.

[12] A. Ahadi, Q. Sun, Stress-induced nanoscale phase transition in superelastic NiTi by in situ X-ray diffraction, Acta Mater. 90 (2015) 272–281.

[13] Z. Zhang, X. Ding, J. Sun, T. Suzuki, T. Lookman, K. Otsuka, X. Ren, Nonhysteretic Superelasticity of Shape Memory Alloys at the Nanoscale, Phys. Rev. Lett. 111 (2013) 145701.

[14] D.L. Shan, C.H. Lei, Y.C. Cai, K. Pan, Y.Y. Liu, Mechanical control of electrocaloric response in epitaxial ferroelectric thin films, Int. J. Solids Struct. 216 (2021) 59–67.

[15] Y.Y. Liu, Z.X. Zhu, J.F. Li, J.Y. Li, Misfit strain modulated phase structures of epitaxial Pb(Zr 1-xTix)O3 thin films: The effect of substrate and film thickness, Mech. Mater. 42 (2010) 816–826.

[16] G. Fan, W. Chen, S. Yang, J. Zhu, X. Ren, K. Otsuka, Origin of abnormal multi-stage martensitic transformation behavior in aged Ni-rich Ti-Ni shape memory alloys, Acta Mater. 52 (2004) 4351–4362.

[17] J. Michutta, C. Somsen, A. Yawny, A. Dlouhy, G. Eggeler, Elementary martensitic transformation processes in Ni-rich NiTi single crystals with Ni4Ti3 precipitates, Acta Mater. 54 (2006) 3525–3542.

[18] L. Bataillard, J.E. Bidaux, R. Gotthard, Interaction between microstructure and multiple-step transformation in binary NiTi alloys using in-situ transmission electron microscopy observations, Philos. Mag. A. 78 (1998) 327–344.

[19] Y.L. Hao, H.L. Wang, T. Li, J.M. Cairney, A.V. Ceguerra, Y.D. Wang, Y. Wang, D. Wang, E.G. Obbard, S.J. Li, R. Yang, Superelasticity and Tunable Thermal Expansion across a Wide Temperature Range, J. Mater. Sci. Technol. 32 (2016) 705–709.

[20] L.D. Landau, E.M. Lifshitz, Statistical physics, Pergamon Press, Oxford, 1980.

[21] J.W. Cahn, J.E. Hilliard, Free Energy of a Nonuniform System. I. Interfacial Free Energy, J. Chem. Phys. 28 (1958) 258.

[22] J. Zhu, T. Zhang, Y. Yang, C.T. Liu, Phase field study of the copper precipitation in Fe-Cu alloy, Acta Mater. 166 (2019) 560–571.

[23] A.G. Khachaturyan, Theory of Structural Transformations in Solids, John Wiley & Sons, New York, 1983.

[24] J. Cahn, On spinodal decomposition, Acta Metall. 9 (1961) 795–801.

[25] J.D. Gunton, M.S. Miguel, P.S. Sahni, The Dynamics of First Order Phase Transitions, in: C. Domb, J. Lebowitz (Eds.), Phase Transitions Crit. Phenom., Academic Press, London, 1983: pp. 269–466.

[26] H.H. Wu, A. Pramanick, Y.B. Ke, X.-L. Wang, Real-space phase field investigation of evolving magnetic domains and twin structures in a ferromagnetic shape memory alloy, J. Appl. Phys. 120 (2016) 183904.

[27] H.H. Wu, Y. Ke, J. Zhu, Z. Wu, X.L. Wang, Effects of magnetic frequency and the coupled magnetic-mechanical loading on a ferromagnetic shape memory alloy, J. Phys. D. Appl. Phys. 54 (2021).

[28] L. Jiang, Y. Zhou, Y. Zhang, Q. Yang, Y. Gu, L.Q. Chen, Polarization switching of the incommensurate phases induced by flexoelectric coupling in ferroelectric thin films, Acta Mater. 90 (2015) 344–354.

[29] J. Liu, Y.Y. Wang, Y.-L. Hao, Y.Y. Wang, Z. Nie, D. Wang, Y. Ren, Z. Lu, J. Wang, H. Wang, X. Hui, N. Lu, M.J. Kim, R. Yang, New intrinsic mechanism on gum-like superelasticity of multifunctional alloys, Sci. Rep. 3 (2013) 2156.

[30] J. Zhu, H. Wu, D. Wang, Y. Gao, H. Wang, Y. Hao, R. Yang, T.-Y. Zhang, Y. Wang, Crystallographic analysis and phase field simulation of transformation plasticity in a multifunctional β-Ti alloy, Int. J. Plast. 89 (2017) 110–129.

[31] C.H. Lei, Y. Liu, W. Chen, Formations and evolutions of martensitic tents and tunnels in shape memory alloy thin films, Mech. Mater. 134 (2019) 9–17.

[32] B. Lai, Y. Wang, Y. Shao, Y. Deng, W. Yang, L. Jiang, Y. Zhang, Study on the phase

transition dynamics of HfO2-based ferroelectric films under ultrafast electric pulse, J. Phys. Condens. Matter. 33 (2021) 405402.

[33] Y.L. Hao, S.J. Li, S.Y. Sun, R. Yang, Effect of Zr and Sn on Young's modulus and superelasticity of Ti–Nb-based alloys, Mater. Sci. Eng. A. 441 (2006) 112–118.

[34] Y. Yang, P. Castany, M. Cornen, F. Prima, S.J. Li, Y.L. Hao, T. Gloriant, Characterization of the martensitic transformation in the superelastic Ti-24Nb-4Zr-8Sn alloy by in situ synchrotron X-ray diffraction and dynamic mechanical analysis, Acta Mater. 88 (2015) 25–33.

[35] Y.W. Zhang, S.J. Li, E.G. Obbard, H. Wang, S.C. Wang, Y.L. Hao, R. Yang, Elastic properties of Ti–24Nb–4Zr–8Sn single crystals with bcc crystal structure, Acta Mater. 59 (2011) 3081–3090.

[36] J. Zhu, Y. Gao, D. Wang, T.-Y. Zhang, Y. Wang, Taming martensitic transformation via concentration modulation at nanoscale, Acta Mater. 130 (2017) 196–207.

[37] D.L. Moffat, U.R. Kattner, The stable and metastable Ti-Nb phase diagrams, Metall. Trans. A. 19 (1988) 2389–2397.